



Experimental Study on Strain Softening Behaviour of Shear Fracture in Concrete Structures.

Seiichiro Ishihara¹⁾ and Hirozo Mihashi²⁾

1) *Asanuma Corporation, Japan*

2) *Tohoku University, Japan*

ABSTRACT

With the aim of examining the shear transfer mechanism and the strain softening behaviour of shear fracture process in concrete structures, shear tests were performed. Also the differences in the shear transfer mechanism and the strain softening behaviour of the shear fracture process between construction joints of different degrees of surface roughness and unjointed concrete structures was investigated. As a result, it has become clear that the shear fracture process is subdivided into approximately four stages: pre-crack initiation stage, crack propagation stage, transition stage, and interlocking stage. Strain softening behaviour of the shear fracture was observed in the crack propagation stage indirectly.

1 INTRODUCTION

The mechanism of nonlinear behaviour in concrete structures mainly depends on cracking behaviour associated with strain softening. Therefore it is necessary to examine strain softening behaviour of fracture process to make clear the mechanism of nonlinear behaviour. The amount of experimental data on the mechanical properties of shear fracture process zone is too limited. For making clear the shear transfer mechanism and strain softening behaviour of the fracture process zone, shear tests were performed. Those tests were loaded very slowly to observe the process of crack initiation and propagation. Also the difference of shear transfer mechanism and strain softening behaviour of the shear fracture process between construction joints and unjointed concrete structures was investigated.

2 EXPERIMENTAL PROGRAM

2.1 Test Specimens

Two series (A and B) of tests were performed. The fundamental mechanism of shear transfer was confirmed by the test series A. The test series B was added for examining in detail the state of crack propagation. Details of each test specimen

used in the pure shear test are given in Table 1. The schematic diagrams of test specimens are shown in Fig. 1. There are four degrees of roughness of construction joints: plain, a little rough, rough, and very rough. The specimens of each test had the same fundamental configuration. The main differences of each test were the shear plane in the area and the loading speed. The differences of each test series is shown in Table.2. The specimen and loading system of our tests are shown in Fig. 2. Instead of embedded reinforcing bars, four steel internal restraint bars passing through the inner sheaths are insetted to apply the axial compressive force upon the crack plane by pushing. At the start of the shear test, the steel internal restraint bars had no applied axial compressive force. Dowel action and unnecessary shear resistance due to the steel internal restraint bars were avoided by making the sheaths 5mm larger in diameter and placing the bars in the center thereof.

2.2 Concrete

The Mix proportion of concrete in test series A and B is given in Table 3. Six days

Table 1. Details of specimen

A series			B series		
Type of Const.Joint	Degree of Roughness of Const.Joint	Numbers	Type of Const.Joint	Degree of Roughness of Const.Joint	Numbers
Const.joint-UP (Upper)	A little rough	2	Const.joint-LW (Lower)	Plain	3
	Rough	3		A little rough	2
	Very rough	3	Unjointed	-	3
Const.joint-LW (Lower)	Rough	3			
	Very rough	2			
Unjointed	-	3			

Table 2. The difference between test series A and B

Test Series	Shear plane in the area	Loading speed	Hinge	Reinforcement ratio of restraint steel bars
A	10cm×10cm	0.02 mm / min	Only upper part	1.34 %
B	9cm×9cm	0.005 mm / min	Upper and lower part	1.34 %

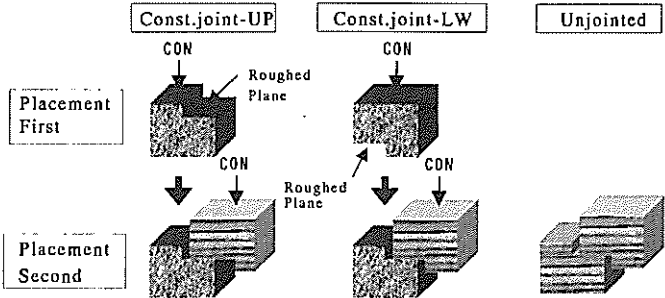


Fig.1. Schematic diagram of test specimens

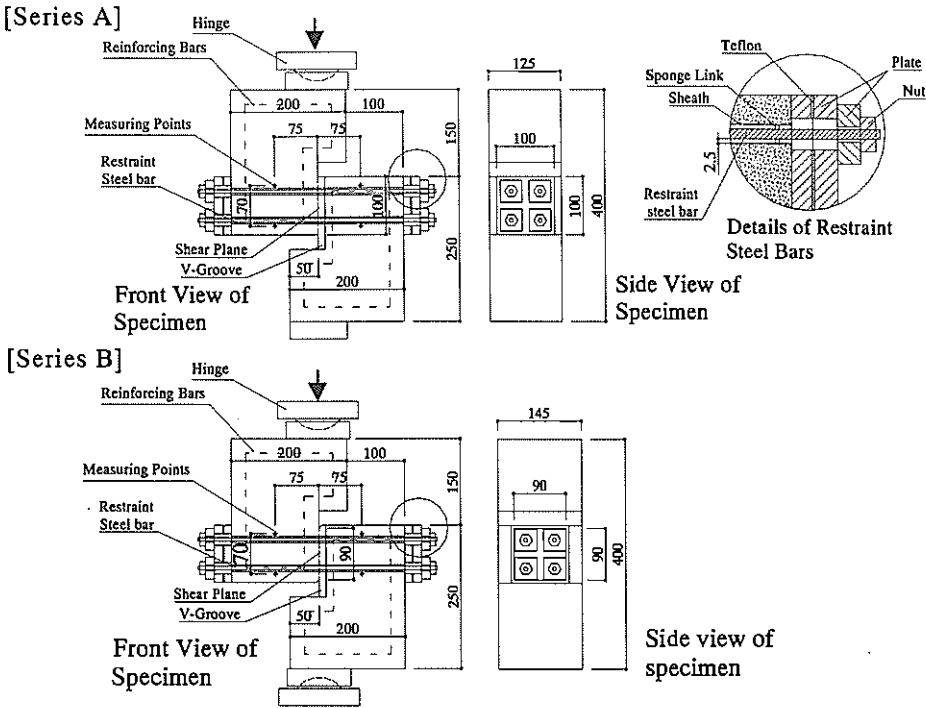


Fig. 2. Specimen and loading system

after placing concrete in the first portion, the joint surface was roughened. Seven days after roughening, the second portion was placed. Unjointed concrete specimens were cast at the same time as the second portion. The material properties of the concrete in each test are shown in Table 4.

2.3 Measuring of Concrete Surface Roughness

The concrete surface roughness was measured at intervals of about 0.1mm using a laser displacement gauge. The method of measuring the concrete surface is shown in Fig. 3. Definition of concrete surface roughness (R_a) is shown in Fig. 4.

2.4 Testing Procedure

The shear displacement rate of test series A was 0.02mm/min, and that of test

Table 3. Mix proportion of concrete

Test series	Type of Cement	G_{max} (mm)	Unit content (kg/m^3)				Chemical Admixture (ℓ/m^3)
			Cement	Water	Fine Aggregate	Coarse Aggregate	
A	NPC*	15	315	189	808	949	0.788
B	NPC*	15	315	189	867	888	0.788

*NPC = Normal Portland Cement

Table 4. Material properties of concrete

	Series A			Series B		
	Compressive Strength (N/mm ²)	Tensile Strength (N/mm ²)	Young's Modulus (×10 ⁴ N/mm ²)	Compressive Strength (N/mm ²)	Tensile Strength (N/mm ²)	Young's Modulus (×10 ⁴ N/mm ²)
First Portion	24.2	2.07	2.3	30.1	2.43	2.38
Second Portion	24.2	2.04	2.32	26.5	2.20	2.31
Unjointed	24.2	2.04	2.32	26.5	2.20	2.31

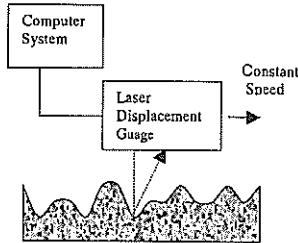


Fig.3 Method of measuring concrete surface roughness

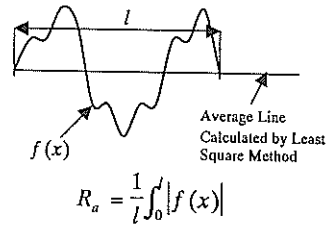


Fig. 4. Definition of concrete surface roughness (Ra)

series B was 0.005mm/min. After passing the peak of the load-shear displacement curve, the displacement rate of each test was increased gradually to 0.06 mm/min. Data sampling speed was approximately once per second.

3 EXPERIMENTAL RESULTS AND DISCUSSION

3.1 Relation Between Shear Stress and Shear Displacement

The relation between shear stress and shear displacement for representative specimens of test series A and B in Table 5 are shown in Fig. 5. Each specimen showed a phased change. A schematic description of the phased change in shear stress and shear displacement is shown in Fig.6.

The phased change was subdivided into approximately four stages. The first was the stage before crack initiation which showed elastic behavior, the second was the stage of crack propagation, the third was a transition stage after crack propagation ended, and the final stage was a stable aggregate interlocking stage. However, there was no clear crack propagation stage in specimen B-1.

Table 5. Test results for representative specimens

Specimen	Type of Joint	Ra (mm)	τ_{ci} (N/mm ²)	τ_{si} (N/mm ²)	τ_{si} / τ_{ci} (%)
A-1	Const.joint-UP	0.61	4.42	0.93	21.0
A-2	Const.joint-UP	2.19	4.73	3.16	66.8
A-3	Unjointed	-	4.43	3.36	75.9
B-1	Const.joint-LW	0.075	4.63	0.70	15.1
B-2	Const.joint-LW	0.45	4.99	2.41	48.3
B-3	Unjointed	-	4.89	4.46	91.2

τ_{ci} : shear stress at cracking initiation
 τ_{si} : shear stress at the start of interlocking stage

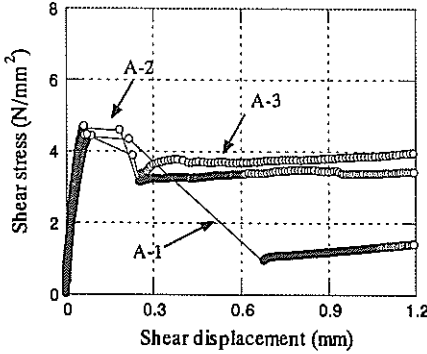
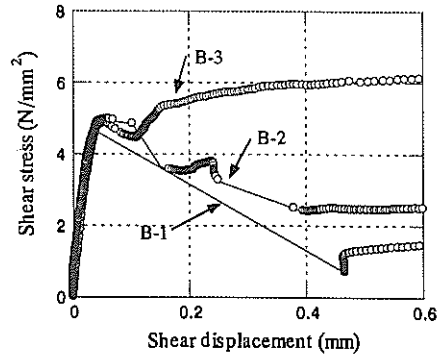


Fig. 5. Shear stress vs. shear displacement of representative specimen



Explanation of stages

- I : Pre-crack initiation stage
- II : Crack propagation stage
- III : Transition stage
- IV : Interlocking stage

Fig. 6. Schematic description of shear stress and shear displacement

3.2 Relation between shear stress and concrete surface roughness

The relation between shear stress at crack initiation $\tau_{ci} / \sqrt{\sigma}$ and concrete surface roughness Ra of each specimen are shown in Fig. 7. The shear stress in construction joints at crack initiation was almost constant although the degree of concrete surface roughness was different. Also, the shear strength of specimens with construction joints was nearly the same as that of unjointed specimens. Furthermore, there was no difference between Const.joint-UP and Const.joint-LW.

The relation between shear stress at the start of interlocking stage $\tau_{si} / \sqrt{\sigma}$ and Ra of each specimen is shown in Fig. 8. The difference of shear stress owing to the degree of surface roughness was revealed in the stage after crack initiation.

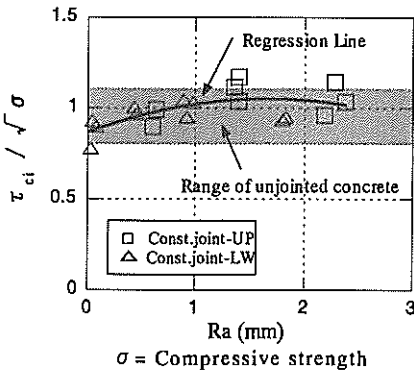


Fig. 7. $\tau_{ci} / \sqrt{\sigma}$ vs. Ra

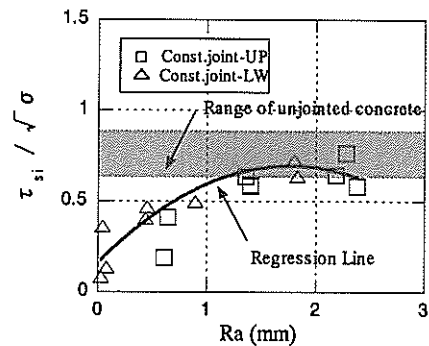


Fig. 8. $\tau_{si} / \sqrt{\sigma}$ vs. Ra

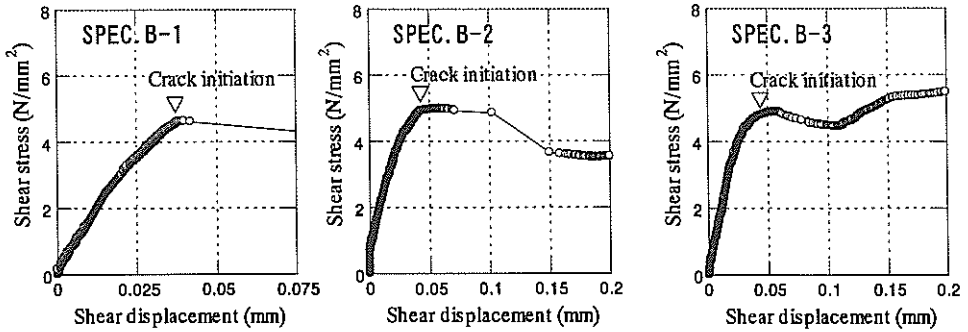


Fig.9. Details of shear stress vs. shear displacement in crack propagation stage

3.3 Mechanism of shear crack propagation

In this experiment, the stage on which the shear crack propagated after crack initiation was confirmed. We were able to detect the existence of the crack propagation stage in the tests on series A, but were unable to observe the process of crack propagation stage adequately. To examine crack propagation in detail, shear tests in series B were loaded more slowly than series A. The relation between shear stress and shear displacement in the crack propagation stage of specimens B-1, B-2 and B-3 are shown in detail in Fig.9. Crack propagation was observed to be gradual in specimens B-2 and B-3. However we were unable to observe a clear propagation stage in specimen B-1. Since the degree of concrete surface roughness of the construction joint in specimen B-1 was plain, the crack propagation was too rapid to be measured.

In the crack propagation stage, shear stress was almost constant in the specimens of both series except for specimen B-1, although shear displacement increased. In this stage two mechanisms may be working simultaneously: one is "shear transfer" due to aggregate bridging; the other is "shear strain softening" in which shear stress decreases with increasing shear strain of the fracture process zone.

We assumed that shear transfer in this stage is governed not by the magnitude of

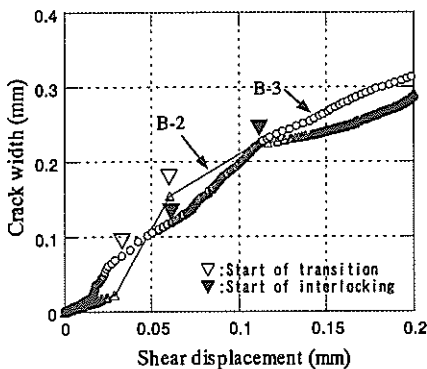


Fig.10. Crack width vs. shear displacement

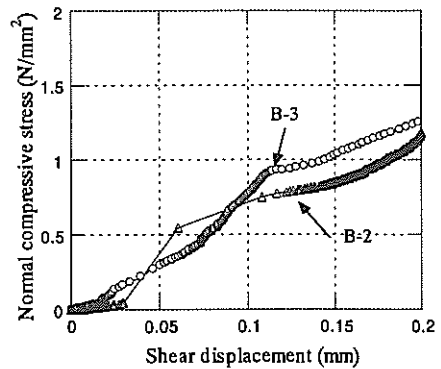


Fig.11 Normal compressive stress vs. crack width

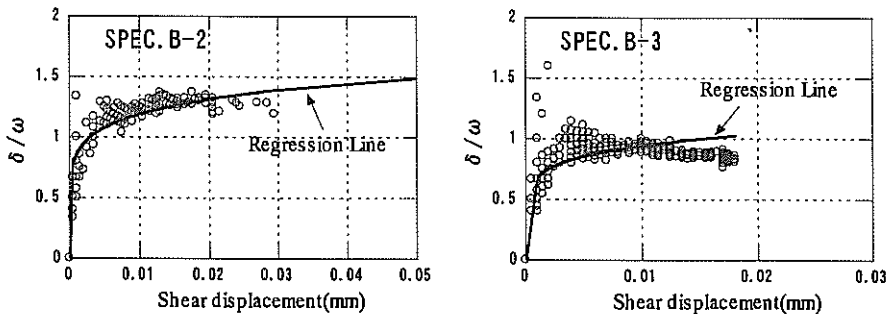


Fig.12. Ratio of shear displacement over crack width vs. shear displacement

crack width but by the ratio of shear displacement to crack width, because the crack width in the crack propagation stage is much smaller than the aggregate size. Paulay and Loeber's experiments proved that the maximum shear stress of cracked concrete doesn't depend on the crack width but has almost constant value. Also Okamura and Maekawa showed from their experiments that under monotonic loading paths, the shear stress transferred across a crack is governed not by the magnitude of crack width but by the ratio of shear displacement to the crack width. Thus, the model proposed by Okamura and Maekawa (1991) was adopted as the model for shear transfer.

The model is described in Table 6 (A). We assumed that shear transfer starts from crack initiation and that transferred shear stress reaches the maximum value at the end of crack propagation. The relation between crack width and shear displacement

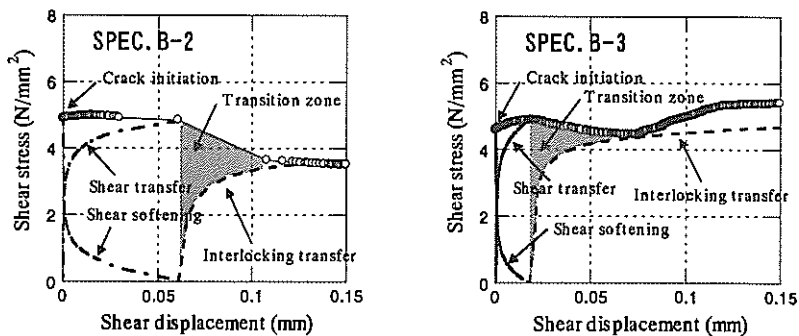


Fig.13. Mechanism of crack propagation

Table 6. Model for shear transfer and interlocking stage

(A) Model of shear transfer	(B) Model of interlocking
$\tau = \frac{m_1 \psi^2}{1 + \psi^2}$	$\tau = \frac{m_2 \phi^{3/5}}{1 + \phi^{3/5}}$
where $\psi = \delta / \omega$ δ : Shear displacement ω : Crack width fc: Compressive strength $m_1 = 2.3 \text{ fc}^{1/3}$ (SPEC.B-2) $3.2 \text{ fc}^{1/3}$ (SPEC.B-3)	where $\phi = \delta / \omega(\delta)$ δ : Shear displacement $\omega(\delta)$: Crack width fc: Compressive strength $m_2 = 2.4 \text{ fc}^{1/3}$ (SPEC.B-2) $3.8 \text{ fc}^{1/3}$ (SPEC.B-3)

after crack initiation in specimens B-2 and B-3 is shown in Fig.10. The Relation between crack width and normal compressive stress after crack initiation is shown in Fig.11. The relation between the ratio of shear displacement to crack width δ/ω and shear displacement on the propagation stage is shown in Fig.12. Although the value of δ/ω showed diversity, it increased in a similar way to a regression line with increase of shear displacement. The value of regression was adopted for δ/ω of this analytical model. The coefficient m_1 of this model is related to contact density and contact area of the crack surface. The coefficient was determined as to match with shear test results. The analytical results of shear transfer by this model are shown in Fig. 13.

The difference between measured total shear stress and the analytical results of shear transfer could be caused by shear strain softening. In the propagation stage, the strain exceeded a limit as a result of the accumulation of micro-cracking. Hence shear strain softening occurred with increasing strain while stress decreased. It is supposed that the shear strain softening and shear transfer occur simultaneously just after crack initiation.

After crack propagation ends up, the total mechanism shifted in another new equilibrium system. In the transition stage, unjointed specimens display less shear displacement compared to construction joints. A model for the interlocking shear transfer is described in Table 6 (B). The coefficient m_2 of this equation was determined according to experimental results. The analytical results of interlocking transfer calculated by this model are shown in Fig.13. The hatched area in Fig. 13 is the transition zone.

4 CONCLUSIONS

The following conclusions were obtained.

- 1.The shear transfer mechanism is subdivided into four stages: pre-crack initiation stage, crack propagation stage, transition stage, and interlocking stage.
- 2.In the crack propagation stage, two mechanisms may be working simultaneously. One mechanism is "shear strain softening", the other is "shear transfer". From the examination of the crack propagation stage in detail, the existence of "shear strain softening" was suggested indirectly.
3. The shear strength of specimens with construction joints at crack initiation was nearly the same as that of unjointed. The difference in shear transfer between construction joints and unjointed or between differing degrees of surface roughness of construction joints is caused by the difference after crack initiation.

5 REFERENCES

- Ishihara, S., Mihashi, H. and Rokugo, K., "Experimental Study on The Mechanical Behavior of Construction Joints in Concrete Structures," Fracture Mechanics of Concrete Structures, pp.783-792, Aedificatio Publishers,1998.
- Paulay, T. and Loeber, P.J., "Shear transfer by Aggregate Interlock," Special publication , ACI, SP-42, Vol. 1 ,1974, pp.1-15.
- Li, B. and Maekawa, K., "Stress transfer constitutive equation for cracked plane density function," Concrete Journal of JCI, Vol. 26 ,No.1,1988, pp.123-137.